Approximate scaling formula for ion–ion mutual neutralization rates

A. P. Hickman

Citation: The Journal of Chemical Physics **70**, 4872 (1979); doi: 10.1063/1.437364
View online: https://doi.org/10.1063/1.437364
View Table of Contents: http://aip.scitation.org/toc/jcp/70/11
Published by the American Institute of Physics

Approximate scaling formula for ion–ion mutual neutralization rates

A. P. Hickman

Molecular Physics Laboratory, SRI International, Menlo Park, California 94025
(Received 15 December 1978)

A complex potential model is used to treat the mutual neutralization of positive and negative ions. The model is used to examine neutralization by the charge transfer mechanism and also by internal excitation leading to capture. It is found that electron transfer is the dominant process for simple ions and small hydrated ions. The numerical results of the theory have been parameterized in terms of the reduced mass of the collision and the electron affinity of the electron donor. This procedure yields an approximate scaling formula that fits a wide range of experimental data to an accuracy of about ±30%.

I. INTRODUCTION

This paper concerns the theoretical study of the mutual neutralization reaction between positive and negative ions. This general class of reactions is of the form

$$X^+ + Y^- \rightarrow X^* + Y . \quad (1)$$

where X^+ and Y^- are charged species that may range in size and complexity from simple ions such as H^-, O^-, O_2^+, NO^+, or NO_3^- to hydrated or "cluster" ions such as $H_3O^+ \cdot (H_2O)_n$ or $NH_4^+ \cdot (NH_3)_n$. The hydration or cluster number n may range from 1 to 6 or even larger. Typically one of the neutral products of the reaction is in an excited state, denoted in Eq. (1) by X^*. This class of reactions is responsible for the final removal of ions at altitudes below 80 km in the ionosphere, and knowledge of the rate constants is of considerable practical importance.

The purpose of the present work is to develop a model that can be used to estimate rate constants for a wide variety of reactions of the form (1). Two distinct mechanisms will be incorporated into the model. The first is neutralization by electron transfer, which has been previously studied by Olson.[1] Our treatment of electron transfer is similar to Olson's. However, the present theory is more general because it provides a unified framework within which both electron transfer and internal excitation can be treated. Internal excitation has been proposed[2] as a mechanism leading to a capture reaction and formation of neutral XY. The interaction of the projectile with the target causes a transfer of energy ΔE from the initial translational mode to internal vibrational and rotational modes. If ΔE is greater than the initial relative kinetic energy, the collision partners will be trapped in a large ellipsoidal orbit. One expects that when the target is a large cluster, energy transfer back to translational motion will be unlikely. Over a period of several orbits, each successive close encounter will then lead to greater internal excitation and a more tightly bound orbit. Alternatively, electron transfer could occur during the successive encounters, leading to separated neutral products.

In Sec. II we develop in detail the theoretical model, which is based on treating the loss of ions to the neutralization channels by adding an imaginary part to the potential. The connection with Olson's absorbing sphere model is discussed. Numerical results are presented and discussed in Sec. III. Our calculations indicate that electron transfer is the dominant neutralization mechanism for collisions involving small ions and clustered species with $n \leq 3$. The calculations also yield scaling rules for such collisions. We illustrate the effect of single hydration by comparing in detail collisions of $O^- + NO^+$ and $O^- + NO^+ \cdot H_2O$, and discuss qualitatively the application of the model to larger clusters. Section IV contains concluding remarks.

II. THEORY

A. Complex potential model

In this section we develop a complex potential model to treat ion–ion mutual neutralization. We first consider the case of the electron transfer mechanism, and then show how internal excitations can also be included.

A schematic diagram of the relevant potential curves is shown in Fig. 1. The idea is that charge exchange can occur via a curve crossing from the initial ionic potential to any one of a number of closely spaced states of the form $X^* + Y$. It is assumed that the final states are sufficiently closely spaced that at any separation R of X^+ and Y^-, some final state curve will cross the ini-

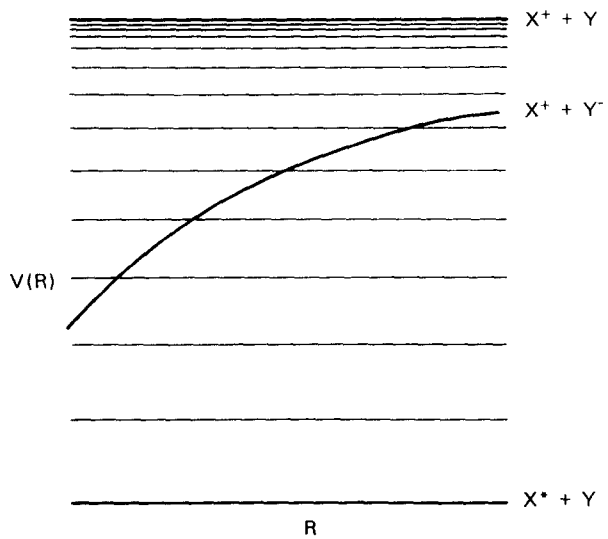

FIG. 1. Schematic diagram of the relevant potential curves for ion–ion mutual neutralization. The state $X^* + Y$ is one of a manifold of closely spaced states indicated by the light lines.

 0021-9606/79/114872-07$01.00

tial state. At this R, the transition occurs predominantly to this particular final state. The matrix element connecting the initial and final states will be denoted by $H_{fi}(R)$. An approximate formula for $H_{fi}(R)$ has been deduced by Olson, Smith, and Bauer[3] by correlating a large number of *ab initio* calculations and experimental results.

Our model consists of treating the closely spaced final states as a continuum, and defining an R-dependent transition probability or width Γ. The function $\Gamma(R)$ gives the rate of transitions out of the initial ionic channel at each R. The dynamics of the collision are treated by adding an imaginary component $-(i/2)\Gamma(R)$ to the potential function $V(R)$ of the ionic channel. [In the present case, $V(R) = -1/R$.] This complex potential model has been used in various other applications[4–6] involving an initial state embedded in a continuum of states, and its application to an initial state crossing a series of discrete but closely spaced states has been discussed by Miller and Morgner.[7] The general conditions necessary for the validity of the model are the following: (1) The final states must be sufficiently closely spaced that transitions may be considered to occur continuously along a trajectory, rather than at isolated curve crossings; (2) the probability of transitions from the neutral channels back to the ionic channel must be negligible. We expect these conditions to be valid in the present case.

We now formulate the model more precisely. We define (in the standard way[8])

$$\Gamma(R) = 2\pi\rho\left|H_{fi}(R)\right|^2 . \tag{2}$$

ρ is the density of final states. For a manifold of final states whose energy levels are given (in a.u.) by a Rydberg formula

$$E_n = -\frac{1}{2n^2} . \tag{3}$$

ρ is easily shown from the work of Miller and Morgner[7] to be

$$\rho = [2(\text{E.A.} + R^{-1})]^{-3/2} , \tag{4}$$

where E.A. is the electron affinity of Y. We adopt Eq. (4) as the definition of ρ even though the electronic energy levels of a complicated molecule may deviate somewhat from Eq. (3).

The matrix element $H_{fi}(R)$ is defined by Olson, Smith, and Bauer[3] and Olson[1] as follows:

$$H_{fi}(R) = 1.044 I_i^{1/2} I_f^{1/2} R^* \exp(-0.857R^*) , \tag{5}$$

where

$$R^* = (I_i^{1/2} + I_f^{1/2})/\sqrt{2} \tag{6}$$

and

$$I_f = I_i + R^{-1} . \tag{7}$$

The quantity I_i is the detachment energy (in a.u.) of the electron being transferred. For ground state negative ions, I_i is just the electron affinity E.A. Formula (5) is estimated by Olson[1] to be valid to about a factor of three.

The probability of electron transfer on a trajectory whose orbital angular momentum is l is given by[5]

$$P_l = 1 - \exp(-2A_l) , \tag{8}$$

where

$$A_l = \int_{R_l}^{\infty} \frac{\Gamma(R)\,dR}{\hbar v_l(R)} \tag{9}$$

and

$$v_l(R) = \left[\frac{2}{m}\left(E + \frac{1}{R} - \frac{(l+\frac{1}{2})^2}{2mR^2}\right)\right]^{1/2} . \tag{10}$$

In this formula E is the collision energy and m is the reduced mass. For trajectories in the Coulomb potential, the classical turning point (distance of closest approach) R_l is given by

$$R_l = (l^2/m)[1 + (1 + 2El^2/m)^{1/2}]^{-1} . \tag{11}$$

The total cross section for neutralization is given by

$$\sigma = \frac{\pi}{k^2}\sum_l (2l+1)P_l , \tag{12}$$

where k^2 is related to the collision energy E by $E = \hbar^2k^2/(2m)$ and to the velocity v by $v = \hbar k/m$. The rate constant α is obtained by taking the appropriate thermal average over a Boltzmann distribution of velocities $f(v, T)$:

$$\alpha(T) = \int_0^{\infty} f(v, T)\sigma(v)v^3\,dv , \tag{13}$$

where

$$f(v, T) = 4\pi\left(\frac{m}{2\pi kT}\right)^{3/2}\exp\left(-\frac{mv^2}{2kT}\right) . \tag{14}$$

For thermal energies, essentially all of the velocity dependence of the cross section Eq. (12) is contained in the $1/k^2$ prefactor. This is because the Coulomb field accelerates particles to velocities many times greater than their initial thermal velocities. To a good approximation, therefore, P_l in Eq. (8) may be considered independent of energy, and R_l in Eq. (11) may be taken to be

$$R_l = l^2/2m . \tag{15}$$

Then if $\bar{v} = (8kT/\pi m)^{0.5}$ is the average velocity at temperature T, it is easily shown that

$$\alpha(T) = \frac{4}{\pi}\bar{v}\,\sigma(\bar{v}) . \tag{16}$$

We now consider the extension of the above model to include neutralization via internal excitation of the target. It is necessary to include terms in the potential corresponding to the internal vibration and rotation of the target. We consider here the case that the target has a dipole moment and a single vibrational coordinate. We will treat the rotational and vibrational excitation using the formulas of semiclassical perturbation scattering (SPS) theory.[9–11]

In the absence of the electron transfer mechanism, the SPS formulas presented by Miller and Smith[10] may be used to calculate the transition probabilities from the initial state $Jj_il_iv_i$ to the final state $Jj_fl_fv_f$. These are

obtained from the T matrix elements, which are written as simple analytic functions of the "average" quantum numbers $\bar{j}=\frac{1}{2}(j_i+j_f)$, etc., and the changes $\Delta j=(j_f-j_i)$, etc.:

$$T=T(J;\bar{j}\,\bar{l}\,\bar{v};\Delta j\Delta l\Delta v)\,. \tag{17}$$

Mukherjee and Smith[11] showed that the total cross section for a particular $(j_iv_i)\to(j_fv_f)$ transition is given by

$$\sigma(j_iv_i\to j_fv_f)=\frac{\pi}{k^2(2j_i+1)}\sum_{\bar{l}}\sum_{\Delta l}\sum_{J}(2J+1)\left|T(J;\bar{j}\,\bar{l}\,\bar{v};\Delta j\Delta l\Delta v)\right|^2, \tag{18}$$

where the sum is over values of l, Δl, and J consistent with angular momentum conservation. (Explicit limits are given by Mukherjee and Smith.[11])

Formula (18) may be written in the form

$$\sigma(j_iv_i\to j_fv_f)=\frac{\pi}{k^2}\sum_{\bar{l}}(2\bar{l}+1)Q_{\bar{l}}(j_iv_i\to j_fv_f)\,, \tag{19}$$

where

$$Q_{\bar{l}}(j_iv_i\to j_fv_f)=\frac{1}{(2j_i+1)(2\bar{l}+1)}\sum_{\Delta l}\sum_{J}(2J+1)\left|T(J;\bar{j}\,\bar{l}\,\bar{v};\Delta j\Delta l\Delta v)\right|^2. \tag{20}$$

The similarity of Eq. (19) to Eq. (12) is evident. If one identified $\bar{l}$ with the angular momentum l in the spherically symmetric case, one may interpret Q_l in Eq. (19) as the probability for a particular (degeneracy averaged) transition on a trajectory whose average orbital angular momentum is $\bar{l}$.

The preceding formulas for $Q_{\bar{l}}$ and $\sigma(j_iv_i\to j_fv_f)$ are based on the assumption that electron transfer cannot occur. If we relax this assumption, then a single collision may lead either to electron transfer, or to internal excitation without electron transfer. The cross section for the former process is given as before by Eq. (12). We define the cross section for the latter process by

$$\tilde{\sigma}(j_iv_i\to j_fv_f)=\frac{\pi}{k^2}\sum_{l}(2l+1)\tilde{Q}_l(j_iv_i\to j_fv_f)\,, \tag{21}$$

where

$$\tilde{Q}_l(j_iv_i\to j_fv_f)=(1-P_l)Q_l(j_iv_i\to j_fv_f)\,. \tag{22}$$

In other words, the probability of internal excitation on a given trajectory depends on the probability that electron transfer does not occur. This assumption is completely analogous to the assumption frequently made in treating spherically symmetric complex potentials, that the real part of the phase shift does not change as the imaginary part of the potential is "turned on."[12] Such a perturbation assumption is consistent with our use of a perturbation approach to the internal excitation.

Formulas (12) and (21) may be used to calculate cross sections for electron transfer and internal excitation of an ionic polar target. In order to calculate the contribution to the total cross section for neutralization it is necessary to make the further assumption that an internal excitation energy ΔE leads invariably to recombination when $\Delta E > E$ (E is the initial translational energy). This is an excellent approximation as long as there are sufficient internal modes to make an energy transfer back to the translational mode unlikely.

B. Relation to absorbing sphere model

The present complex potential approach may be viewed as a generalization of the absorbing sphere model[1] (ASM). The ASM assumes that if the collision partners approach closer than a certain critical distance R_c, then charge transfer via curve crossing occurs with unit probability. R_c depends on the effective mass m and electron affinity E.A., and is the distance at which the matrix element for curve crossing first reaches a particular threshold value. The cross section for neutralization is given by

$$\sigma=\frac{\pi R_c}{E}+\pi R_c^2\,. \tag{23}$$

At thermal energies this is well approximated by

$$\sigma\cong\frac{\pi R_c}{E}\,. \tag{24}$$

The complex potential model assigns a neutralization rate (transition probability per unit time) to each value of the coordinate R. The formulas (8)–(12) correspond to integrating this transition probability along the classical trajectories determined by the potential $V(R)=-1/R$. Formula (11) relating the distance of closest approach and the angular momentum of a Coulomb trajectory enables us to compare the results typically obtained for the complex potential model for P_l [Eq. (8)] with the corresponding prediction of the absorbing sphere model. The comparison is shown schematically in Fig. 2. The ASM gives a step function whose discontinuity is at $l=(2mR_c)^{1/2}$, whereas the complex potential model tends to smooth out the discontinuity.

The use of an R-dependent transition probability makes the present model somewhat more flexible than the ASM. This flexibility may be especially important when one or both of the ionic species are hydrated. The qualitative discussion in Sec. III B shows that the ener-

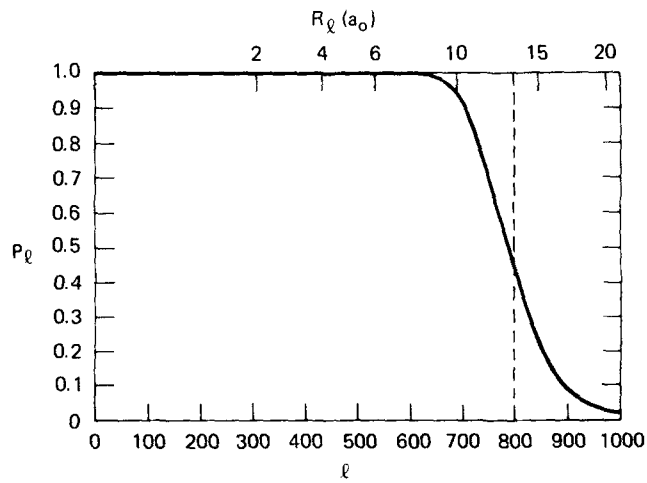

FIG. 2. Schematic illustration of the neutralization probability as a function of orbital angular momentum l or classical turning point $R_l=l^2/2m$, for the complex potential model (solid line) and the absorbing sphere model (dashed line).

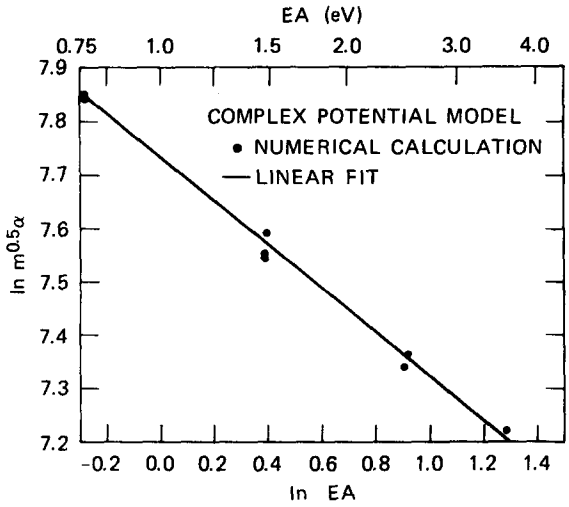

FIG. 3. Demonstration that the numerical results of the complex potential model (points) may be approximately fit by a straight line on an appropriate log–log plot, leading to the power law dependence of Eqs. (25) and (28). E.A. is given in eV, m in a.u., and α in 10^{-8} cm^3/s.

getics of cluster formation imply that $\Gamma(R)$ should be zero for values of R less than some R^*, where R^* will depend on the size of the cluster. For sufficiently large clusters, R^* may be comparable to R_c. In this case, the probability of neutralization by the curve crossing mechanism would be drastically reduced. For such a large cluster, one might expect the internal excitation mechanism to be much more important. The complex potential model, with a Γ related to cluster size, provides a consistent framework for examining the collision process as a function of cluster size.

III. RESULTS AND DISCUSSION

A. Predicted scaling behavior

We have found that the results of the complex potential model for a wide variety of systems can be summarized by a simple scaling rule. Here we discuss how this rule was obtained.

It was first determined that the electron transfer mechanism was much more important than internal excitation for simple ions and small clusters. When only the former mechanism is included, the numerical calculation of the rate constant α for any particular system depends only on m and E.A. We then sought to express the results of all the numerical calculations by a formula of the form

$$\alpha(T) \propto (T/300\ \mathrm{K})^{-0.5} m^{-0.5} (\mathrm{E.A.})^{\lambda} . \tag{25}$$

The $T^{-0.5}$ behavior arises whenever the cross section varies as v^{-2}. This behavior was obtained by Olson in the ASM, and was verified in the present case by direct numerical calculation. The $m^{-0.5}$ behavior was also observed in the calculations. It is easily understood by returning to the ASM, which predicts

$$\alpha \sim \bar{v}\sigma(\bar{v}) = \bar{v}\,\frac{\pi R_c}{E} . \tag{26}$$

Since $E \sim \frac{1}{2} m\bar{v}^2$ and $\bar{v} = (8kT/\pi m)^{0.5}$,

$$\alpha \propto \frac{R_c}{m^{0.5} T^{0.5}} . \tag{27}$$

However, our examination of the absorbing sphere model has shown that R_c depends most strongly on E.A., and only logarithmically on m. We therefore expect that the dependence of α on m and E.A. might be approximated by a power law as in Eq. (25). If this formula is reasonable, then a log–log plot of $\alpha m^{0.5}$ (at $T = 300$ K) vs E.A. will give a straight line of slope λ. Figure 3 shows that such a plot is nearly linear. The slope is determined by a least squares fit to be $\lambda = -0.4$. We therefore obtain the following formula

$$\alpha^{-1} = C(T/300\ \mathrm{K})^{0.5} m^{0.5} (\mathrm{E.A.})^{0.4} . \tag{28}$$

If the units of α, m, and E.A. are cm^3/s, a.u., and eV, respectively, then $C = 4.38 \times 10^4$.

Figure 4 and Table I show that Eq. (28) provides a simple correlation of a wide range of data.[13–17] Considering that the basic formula for $H_{fi}(R)$ was only expected to be accurate to a factor of three, and that the data range from collisions of H^+ and H^- to $H_3O^+ \cdot (H_2O)_3$ and NO_3^-, the approximate scaling rule must be considered remarkably successful.

B. Qualitative discussion of the effects of clustering

The energetics of cluster formation have been previously discussed,[2] and in some cases quantitative calcu-

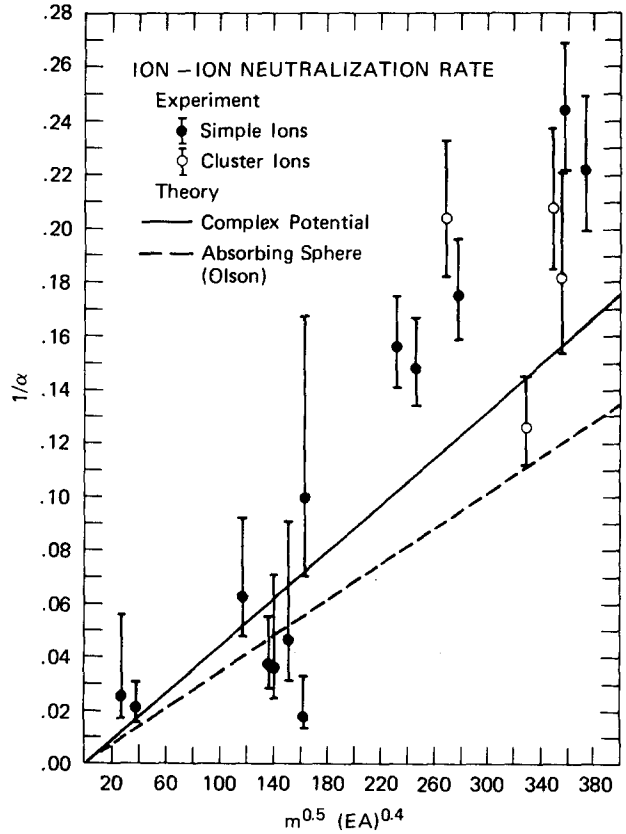

FIG. 4. Comparison of the scaling law, Eq. (28), and experimental data. α is calculated at $T = 300$ K. E.A. is given in eV, m in a.u., and α in 10^{-8} cm^3/s. The data is tabulated for reference in Table I.

TABLE I. Details of the experimental data plotted in Fig. 4. Units are as in Fig. 4.

Ions	$m^{0.5}(\text{E.A.})^{0.4}$	α	Reference
$H^+ + H^-$	27	39 ± 21	13
$H_2^+ + D^-$	38	47 ± 15	17
$N_2^+ + O_2^-$	118	16 ± 5	14
$H^+ + O^-$	137	26 ± 8	13
$O^+ + O^-$	142	27 ± 13	13
$Na^+ + O^-$	153	21 ± 10	15
$NO^+ + O^-$	162	49 ± 20	15
$O_2^+ + O^-$	164	10 ± 4	15
$NO^+ + NO_2^-$	232	6.4 ± 0.7	16
$NH_4^+ + Cl^-$	247	6.7 ± 0.7	16
$NH_4^+ \cdot (NH_3)_2 + NO_2^-$	270	4.9 ± 0.6	16
$NO^+ + NO_3^-$	278	5.7 ± 0.6	16
$NH_4^+ \cdot (NH_3)_2 + Cl^-$	329	7.9 ± 1.0	16
$H_3O^+ \cdot (H_2O)_3 + Cl^-$	350	4.8 ± 0.6	16
$H_3O^+ \cdot (H_2O)_3 + NO_3^-$	356	5.5 ± 1.0	16
$CClF_2^+ + Cl^-$	359	4.1 ± 0.4	16
$CCl_3^+ + Cl^-$	375	4.5 ± 0.5	16

lations have been carried out.[18,19] This section discusses the application of the complex potential model to larger clusters.

In general, one expects that the addition of successive waters of hydration will lower the energy of the ion pair state relative to the corresponding neutrals.[2] The situation is illustrated by the schematic diagram in Fig. 5. The energy of $X^+ \cdot H_2O$ is lower than that of X^+ and an infinitely separated H_2O because of the charge dipole and polarization interactions. In contrast, one expects the energy of $X^* \cdot H_2O$, at the equilibrium separation of $X^+ \cdot H_2O$, to be slightly higher than the energy of X^*.

The curve $X + Y^*$ in Fig. 5 denotes the lowest state to which charge transfer can occur. Because of the stabilizing effect of clustering, discussed in the preceding paragraph, this asymptote moves closer and closer to the ionic state as the cluster size increases. In the context of the complex potential model, we may interpret this to mean that $\Gamma(R)$ should be nonzero only for $R \geq R^*$. An estimate previously used is that each water of hydration moves the two asymptotes 1 eV closer together.[2] If this is the case, then R^* is given (in a.u.) by

$$1/R^* = W - n/27.2 \ . \tag{29}$$

n is the hydration number, and W is the energy difference (in a.u.) between the asymptotes $X^- + Y^+$ and $X + Y^*$ and may be crudely estimated by

$$W \cong \text{I.P.}(Y) - \text{E.A.}(X) \ ; \tag{30}$$

that is, the difference between the ionization potential of Y and the electron affinity of X. For many species of atmospheric interest, W is in the range 6–8 eV (0.2–0.3 a.u.).

Trial calculations were performed in which $\Gamma(R)$ was set to zero for $R \leq R^* = 10a_0$. The change in the rate constant was negligible (less than 1%), indicating that electron transfer occurs mainly at large R. It is likely that cluster formation would cause a reduction in the matrix element for electron transfer. We found that reducing $\Gamma(R)$ by a factor of 4 caused only about a 25% decrease in the rate constant. Combined with Eq. (29) and our estimate of W, these results suggest that for small clusters ($n \lesssim 3$), hydration does not significantly inhibit electron transfer.

C. The internal excitation mechanism: Calculations for $O^- + NO^+$ and $O^- + NO^+ \cdot H_2O$

The system $O^- + NO^+$ is particularly well suited to the application of the complex potential model because the real part of the potential, both the isotropic and anisotropic parts, can be modelled asymptotically using the dipole moment function[20] of NO^+. Cross sections for rotational and vibrational excitation have been calculated both with and without the imaginary part of the potential, using semiclassical perturbation scattering (SPS) theory. The application of this theory in the case where the dipole moment is a linear function of the vibrational coordinate has been discussed by Miller and Smith.[10] Furthermore, we have constructed a simple model for the geometry of $NO^+ \cdot H_2O$, and have examined the cross sections for excitation of the lowest frequency rotational and vibrational modes. The results allow us to examine the competition between the electron transfer and the internal excitation mechanisms for simple ions, and also to obtain information about the changes that occur with the first hydration.

Figure 6 shows the assumed geometry of the $NO^+ \cdot H_2O$ complex. For simplicity, we assume that the center of charge is at the midpoint of the NO^+, and that the interaction of the oxygen of the water molecule with the N and the other O can be described by a Born–Mayer potential[21] of the form

$$f(X) = A \exp(-BX) \ , \tag{31}$$

where $A = 74.445$ a.u. and $B = 2.006$ a.u. This potential is the geometric mean of the Born–Mayer potentials for neutral O–N and O–O interactions. The internuclear separation of NO^+ is taken to be the unperturbed value $2a = 2.00a_0$. With these assumptions, the equilibrium

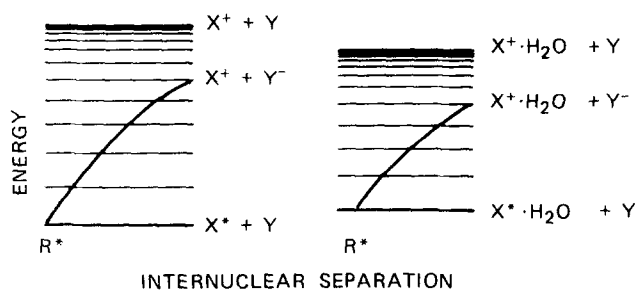

FIG. 5. Schematic diagram showing how hydration tends to lower the energy of an ion pair state relative to the corresponding neutrals. In the text it is argued that for $R < R^*$, $\Gamma(R)$ should be zero.

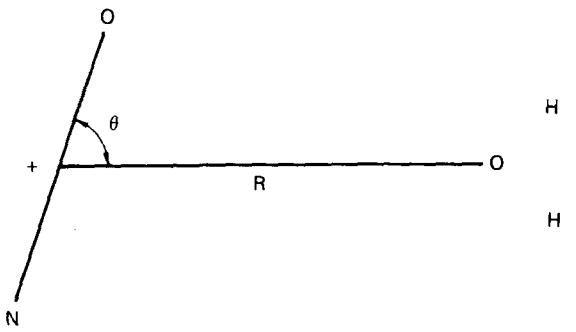

FIG. 6. The geometry assumed for a simple model of $NO^+ \cdot H_2O$ The diagram is not to scale.

geometry will have $\theta = \pi/2$, and R can be determined from the minimum value of the interaction

$$V(R) = 2A \exp[-2B(R^2 + a^2)^{1/2}] - \frac{\mu_0 e}{R^2}, \tag{32}$$

where $\mu_0 = 1.85$ D $= 0.728$ a.u. is the dipole moment of H_2O. For these values of the parameters, the equilibrium value of R is 4.9 a.u., and the well-depth is 0.65 eV.

The above model allows us to calculate the dipole moment (relative to the center of mass), moment of inertia, and rotational energy level spacing of $NO^+ \cdot H_2O$, treating it as a rigid linear molecule. These values are summarized in Table II. The model also allows us to estimate the frequencies of the lowest vibrational or bending modes, and to obtain the dependence of the dipole moment function on the corresponding internal coordinates. We consider both vibration in the R coordinate and bending in the θ coordinate. Estimated frequencies for these modes, assuming they are uncoupled, are also given in Table II.

The results of our calculations may be summarized as follows: For $O^- + NO^+$, the electron transfer mechanism dominates the scattering. Any trajectory that would lead to significant rotational or vibrational excitation in the absence of the width Γ, has a high probability (essentially unity) of electron transfer when Γ is turned on. Also, for those trajectories where the electron transfer probability is small (i.e., large l or large classical turning point), vibrational excitation is much less important than rotational excitation and may be neglected. We have also found that electron transfer is the most important mechanism for $O^- + NO^+ \cdot H_2O$, but that internal excitation may increase the rate constant by about 10% at 300 K. The reason for this is that the cluster has a larger dipole moment than the bare NO^+, and hence rotational excitation can occur for more distant trajectories than for NO^+ alone. The calculations showed that the cross sections for vibrational excitation were considerably smaller than those for rotational excitation for all trajectories not leading to electron transfer. In other words, for the purposes of the complex potential model, the singly hydrated cluster behaves as if it were a rigid rotor.

The final rate constants obtained were as follows. For $O^- + NO^+$, $\alpha(300\text{ K}) = 13.9 \times 10^{-8}$ cm^3/s, essentially all from electron transfer. For $O^- + NO^+ \cdot H_2O$, the rate constant from electron transfer is $\alpha(300\text{ K}) = 13.1 \times 10^{-8}$ cm^3/s; the inclusion of internal excitation changes this to 14.1×10^{-8} cm^3/s.

The extension of the present model, with its detailed assumptions about geometry, to larger clusters is probably not justified without rigorous structure calculations. A few general comments may be pertinent, however. The addition of more water molecules will probably decrease, not increase, the total dipole moment, since some cancellation could be expected to occur. This suggests that large rotational excitation due to distant trajectories may be important only for single (or un-) hydrated ions. The large clusters will have a greater number of internal modes that can be excited by direct impact. Previous discussion has indicated that electron transfer may not occur at close distances for these larger clusters. It may be that at small distances neutralization occurs instead with high probability by the internal excitation mechanism.

IV. CONCLUSIONS

We have presented a theory of ion–ion mutual recombination based on modelling the loss of particles from the initial channel to a manifold of final channel by adding an imaginary part to the Coulomb potential. We have examined the relative importance of competing mechanisms, and have found that the electron transfer process accounts for at least 80% of the rate constant in the cases considered. The results of the theory have been parameterized, and provide a useful and reasonably accurate correlation of a wide range of experimental data.

This correlation formula, Eq. (28), predicts a small decrease in the neutralization rate as the size of the positive ion cluster increases. This effect is due entirely to the change in the effective mass of the relative motion. However, our more detailed study of collisions of hydrated NO^+ with O^- showed a net increase in the rate as the hydration number increased from zero to one,

TABLE II. Values of the molecular parameters of NO^+ and $NO^+ \cdot H_2O$ used in the calculations. Note that the vibrational coordinate of NO^+ is the N–O distance; that of $NO^+ \cdot H_2O$ is the coordinate R shown in Fig. 6, with NO at its equilibrium value.

Parameter	NO^+	$NO^+ \cdot H_2O$
Rotational constant (cm^{-1})	1.99	0.22
Moment of inertia (g cm^2)	1.465×10^{-39}	1.29×10^{-38}
Equilibrium value of vibrational coordinate, R_0 (a_0)	2.0	4.9
Well-depth (eV)		0.65
Equilibrium value of dipole moment relative to c.m., $\mu_0 = \mu(R_0)$, (a.u.)	0.313	1.13
Dipole derivative $\mu'(R_0)$ (a.u.)	0.392	0.375
Vibrational frequency (a.u.) ω_v	0.011	$\sim 9.1 \times 10^{-4}$
Bending frequency (a.u.) ω_b		$\sim 2.1 \times 10^{-4}$

because of the increased probability of internal excitation. It is felt that these results cannot be interpreted to indicate any general trend of neutralization rates as a function of cluster size. They appear only to suggest that the rates for small clusters are not substantially different from the rates for the corresponding bare ions.

ACKNOWLEDGMENTS

The author wishes to acknowledge helpful conversations with D. L. Heustis, J. R. Peterson, R. E. Olson, and F. T. Smith. This research was supported by the Air Force Geophysics Laboratory under Contract No. F19628-75-C-0050.

[1]R. E. Olson, J. Chem. Phys. 56, 2979 (1972).
[2]R. A. Bennett, D. L. Huestis, J. T. Moseley, D. Mukherjee, R. E. Olson, S. W. Benson, J. R. Peterson, and F. T. Smith, ARCRL-TR-74-0417, Air Force Cambridge Research Laboratory, Hanscom, MA, 1974 (unpublished).
[3]R. E. Olson, F. T. Smith, and E. Bauer, Appl. Opt. 10, 1848 (1971).
[4]N. F. Mott and H. S. W. Massey, *The Theory of Atomic Collisions*, 3rd ed. (Clarendon, Oxford, 1965), pp. 184–186.
[5]W. H. Miller, J. Chem. Phys. 52, 3563 (1970).
[6]A. P. Hickman and H. Morgner, J. Phys. B 9, 1765 (1976).
[7]W. H. Miller and H. Morgner, J. Chem. Phys. 67, 4923 (1977).
[8]W. H. Miller, Chem. Phys. Lett. 4, 627 (1970).
[9]F. T. Smith, D. L. Huestis, D. Mukherjee, and W. H. Miller, Phys. Rev. Lett. 35, 1073 (1975).
[10]W. H. Miller and F. T. Smith, Phys. Rev. A 17, 939 (1978).
[11]D. Mukherjee and F. T. Smith, Phys. Rev. A 17, 954 (1978).
[12]Z. F. Wang, A. P. Hickman, K. Shobatake, and Y. T. Lee, J. Chem. Phys. 65, 1250 (1976).
[13]J. R. Peterson, W. H. Aberth, J. T. Moseley, and J. R. Sheridan, Phys. Rev. A 3, 1651 (1971).
[14]W. H. Aberth and J. R. Peterson, Phys. Rev. A 1, 158 (1970).
[15]J. T. Moseley, W. H. Aberth, and J. R. Peterson, J. Geophys. Res. 77, 255 (1972).
[16]D. Smith, M. J. Church, and T. M. Miller, J. Chem. Phys. 68, 1224 (1978).
[17]J. T. Moseley, R. E. Olson, and J. R. Peterson, Case Studies At. Phys. 5, 1 (1975).
[18]M. D. Newton and S. Ehrenson, J. Am. Chem. Soc. 93, 4971 (1971).
[19]M. D. Newton, J. Chem. Phys. 67, 5535 (1977).
[20]F. P. Billingsley, Chem. Phys. Lett. 23, 160 (1973).
[21]A. A. Abrahamson, Phys. Rev. 178, 76 (1969).